Growth and morphology of Er-doped GaN on sapphire and hydride vapor phase epitaxy substrates

R. Birkhahn, R. Hudgins, D. Lee, and A. J. Steckl[a)]
Nanoelectronics Laboratory, University of Cincinnati, Cincinnati, Ohio 45221-0030

R. J. Molnar
Massachusetts Institute of Technology, Lincoln Laboratory, Lexington, Massachusetts 02173

A. Saleh
Charles Evans and Associates, Sunnyvale, California 94086

J. M. Zavada
U.S. Army Research Office, Research Triangle Park, North Carolina 27709

(Received 5 October 1998; accepted 18 February 1999)

We report the morphological and compositional characteristics and their effect on optical properties of Er-doped GaN grown by solid source molecular beam epitaxy on sapphire and hydride vapor phase epitaxy GaN substrates. The GaN was grown by molecular beam epitaxy on sapphire substrates using solid sources (for Ga, Al, and Er) and a plasma gas source for N_2. The emission spectrum of the GaN:Er films consists of two unique narrow green lines at 537 and 558 nm along with typical Er^{3+} emission in the infrared at 1.5 μm. The narrow lines have been identified as Er^{3+} transitions from the $^2H_{11/2}$ and $^4S_{3/2}$ levels to the $^4I_{15/2}$ ground state. The morphology of the GaN:Er films showed that the growth resulted in either a columnar or more compact structure with no effect on green light emission intensity. © *1999 American Vacuum Society.* [S0734-211X(99)06303-9]

The optical properties of rare earth (RE) elements (such as Nd, Er, Pr) have led to many important photonic applications, including solid state lasers, telecommunications (optical fiber amplifiers, fiber lasers), optical storage devices, displays. In most of these applications the host materials for the REs were various forms of oxide and nonoxide glasses. The emission can occur at visible or infrared (IR) wavelengths depending on the electronic transitions of the selected RE element and the excitation mechanism. Semiconductors doped with REs such as Pr and Er have exhibited only the lowest excited state as an optically active transition. However, the presence of these transitions at IR wavelengths (1.3 and 1.54 μm) coincident with minima in the optical loss of silica-based glass fibers utilized in telecommunications combined with the prospect of integration with semiconductor device technology has sparked considerable interest.

The III–N semiconducting compounds are of particular interest as hosts for REs because of their direct band gap and high level of optical activity even under conditions of rather high defect density, which would quench emission in other smaller-gap III–V and wide-gap II–VI compounds. Examples of other RE-doped wide band gap semiconductors (WBGS) which have been reported include GaP,[1] SiC,[2] and III–V compounds.[3] Advantages of WBGS over other semiconductors and glasses include chemical stability, carrier generation (to excite the rare earths), and physical stability over a wide temperature range. The doping of III nitrides (GaN, AlN) with Er by molecular beam epitaxy (MBE) and metal-organic chemical vapor deposition (MOCVD) both during growth and postgrowth by ion implantation has been reported.[4–11] The successful *in situ* incorporation[12–14] of Er into AlN and GaN by MBE and its IR emission characteristics have been reported by other groups. None of these articles in the literature report emission in the visible range from Er-doped III-nitrides. Recently, our group has reported[15–18] the *in situ* incorporation of Er into GaN by MBE on both sapphire and silicon leading to room temperature visible and IR emission by both photoluminescence and electroluminescence (EL). In GaN:Er, besides the commonly measured 1.5 μm emission, we observed two narrow and very strong green lines at 537 and 558 nm, corresponding to higher level Er^{3+} transitions. In this article, we present information on the structural properties of the GaN:Er films on both sapphire and hydride vapor phase epitaxy (HVPE) GaN substrates grown at MIT Lincoln Laboratory.

We have grown Er-doped GaN films in a Riber MBE-32 system directly on *c*-axis sapphire and on 20-μm-thick GaN on sapphire grown by HVPE. Solid sources were employed to supply the Ga (7N purity), Al (6N), and Er (3N) fluxes, while an SVTA radio-frequency (rf)-plasma source was used to generate atomic nitrogen. Prior to insertion into the MBE, the sapphire was cleaned in acetone and methanol and rinsed in DI water. The HVPE GaN was cleaned in acetone, methanol, and dipped in 10% HF. The sapphire substrate was initially nitrided at 750 °C for 30 min at 400 W rf power with a N_2 flow rate of 1.5 sccm, corresponding to a chamber pressure of mid-10^{-5} Torr. An AlN buffer layer was then grown at 550 °C for 10 min with an Al beam pressure of 2.3×10^{-8} Torr (cell temperature of 970 °C). Growth of the Er-doped GaN proceeded at 750 °C for 3 h with a constant Ga beam pressure of 8.2×10^{-7} Torr (cell temperature of 922 °C). In the case of the HVPE GaN, no nitridation or

a)Electronic mail: a.steckl@uc.edu

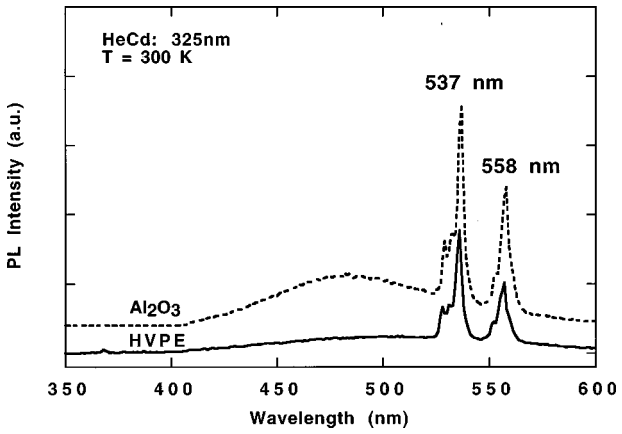

FIG. 1. Visible PL spectrum of Er-doped GaN films grown on sapphire (upper) and HVPE GaN at 750 °C. The Er cell temperature for both films was 1100 °C. The PL is performed at room temperature with the He–Cd laser line at 325 nm.

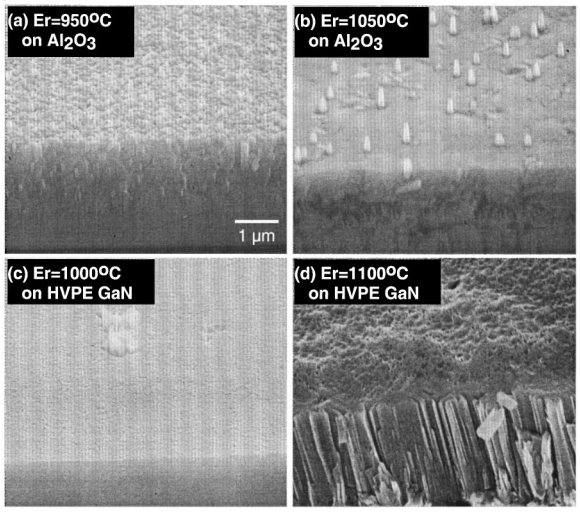

FIG. 2. SEM photos of GaN:Er films on sapphire (a),(b) and HVPE GaN (c),(d).

buffer layer was used. The Er cell temperature was varied from 900 to 1100 °C. The resulting GaN film thickness was nominally 2.4 μm giving a growth rate of $\sim$0.8 μm/h, as measured by scanning electron microscopy (SEM) and transmission spectroscopy. Additionally, two samples, one grown on sapphire and one on HVPE, were annealed *in situ* immediately after growth at 700 °C in high vacuum conditions. We used both SEM and a Dimension 3100 atomic force microscope (AFM) to examine the surface morphological properties and utilized secondary ion mass spectroscopy (SIMS) and Rutherford backscattering (RBS) to understand the compositional effects.

Photoluminescence (PL) characterization of the thin films was performed with a He–Cd laser excitation source at a wavelength of 325 nm, corresponding to an energy greater than the GaN band gap. Further details on PL experiments can be found elsewhere.[15,16] PL excitation resulted in green emission from the Er-doped GaN films, visible with the naked eye. The room temperature PL is shown in Fig. 1 for a GaN film grown on sapphire and HVPE GaN at 750 °C with the Er cell temperature of 1100 °C. The green emission lines at 537 and 558 nm have been identified as $^2H_{11/2}$ and $^4S_{3/2}$ transitions to the $^4I_{15/2}$ ground state levels in the trivalent Er^{3+} ion. We have also observed[17] the corresponding IR emission.

SEM micrographs of several GaN:Er films grown on Al_2O_3 and HVPE GaN substrates are shown in Fig. 2. The samples grown on sapphire substrates are shown in Figs. 2(a) and 2(b) with the Er cell at 950 °C and 1050 °C, respectively. These two surfaces exhibit very different morphology, yet both show the same green Er-related emission. Figure 2(a) shows a columnar structure with a grain size on the order of 0.2 μm or less, while Fig. 2(b) shows a GaN film with a compact structure and unusual broad and squat spikes protruding from the surface. Spikes similar to Fig. 2(b) have been previously observed[16] in GaN:Er films grown on Si (111). Figures 2(c) and 2(d) show the surface morphology of GaN:Er films grown on HVPE GaN substrates. The GaN film grown on HVPE with the Er cell temperature at 1000 °C [Fig. 2(c)] has a compact structure similar to that grown on sapphire with the Er cell at 1050 °C [Fig. 2(b)], although with smaller spikes and a lower overall spike density on the surface. The sample shown in Fig. 2(d) has had postgrowth *in situ* annealing at 700 °C and it shows a highly columnar structure similar to that in Fig. 2(a). This preliminary annealing was found to have no significant effect on the morphology of the GaN thin films. However, a more comprehensive investigation of the effect of annealing needs to be performed, with variations in anneal temperature, ambient atmosphere, and time. All films grown in this experiment show either of the two growth modes or their combination: (1) columnar films or (2) compact films with spikes. This phenomenon neither appears to be a function of Er flux (cell temperature) nor of whether the sample was annealed.

The difference in the two structures, columnar versus compact, does not appear to significantly effect the PL intensity of the green Er emission. This lack of dependence of Er^{3+} emission on film microstructure indicates that Er incorporates substitutionally in the lattice rather than segregate in the boundaries. Previously, a study[19] was done on the effect of III/V flux and growth temperature on the morphology of GaN on Si (111) substrates. It was found that a N-rich surface produced ''whisker-like nanocrystals,'' while on a Ga-rich surface the growth was ''more compact.'' Growth in a columnar manner is typical for MOCVD[20] GaN with highly oriented grains varying only by a small tilt or twist. For our growth runs, Ga flux and N_2 flow and power were kept constant. It is unclear at present why certain GaN:Er films formed in a compact manner and some grew via columns.

AFM scans were done using a Digital Instruments Dimension 3100 to obtain more quantitative data on the surface morphology and roughness. Several 5 μm square scans were analyzed for average roughness on each of the GaN:Er films. The surface average roughness (R_a) is calculated as one over the area times the integral over a function of x and y deter-

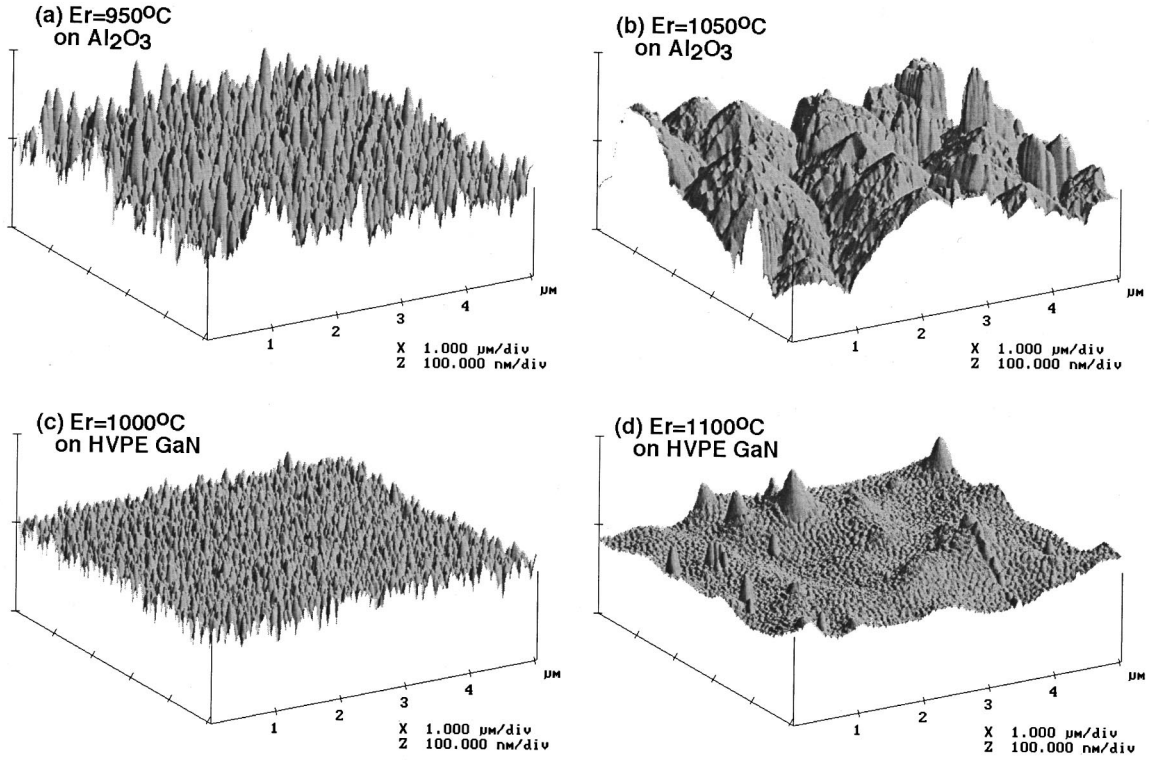

FIG. 3. AFM surface plots of GaN:Er films on sapphire (a),(b) and HVPE GaN (c),(d).

mined as the scan takes place with the initial point of contact as the reference plane:

$$R_a = \frac{1}{L_x L_y} \int_0^{L_y} \int_0^{L_x} F(x,y)\,dx\,dy. \tag{1}$$

Figure 3 shows representative three-dimensional (3D) surface plots from samples grown on sapphire and HVPE. The samples shown in Figs. 3(a) and 3(b) were grown on sapphire with an Er cell temperature of 950 and 1050 °C, respectively. Figure 3(a) shows a uniformly rough area with large spikes and an average roughness (R_a) of 15 nm. Fig. 3(b) exhibits no uniformity and has an average R_a value of 40 nm. The spikes seen on the SEM micrographs are not visible here due to the physical contact of the AFM tip indicating that the spikes are very fragile. Figures 3(c) and 3(d) are scans of the films grown on HVPE. Figure 3(c) shows the best smoothness and uniformity of all the samples in this analysis with an R_a value of 6.4 nm. In Fig. 3(d) columnar regions are visible. In the areas of no columns, a roughness of 7.2 nm was measured. When the columns were included, the average R_a value was 10 nm. A compilation of the R_a values are shown in Fig. 4 for the samples grown on sapphire. The general trend is that the surface roughness increases as the Er flux increases. This is not unexpected as the GaN lattice changes or deforms to accept a higher Er concentration.

SIMS was performed to determine the concentration of Er and unintentional impurities present and the doping profile. Figure 5 shows a representative Er concentration profile for the sapphire substrate (Er cell = 1100 °C) demonstrating that incorporation was constant throughout growth. This concentration ($\approx 3\times10^{20}$ atoms/cm^3) corresponds to a doping level of $\sim$0.3 at. % (using a GaN density of 8.78×10^{22} atoms/cm^3), the highest we report in this study. A further check on the Er concentration in the sapphire was performed by RBS. This plot is shown in Fig. 6. This demonstrated that at an Er cell temperature of 1050 °C, Er incorporation was 0.2 at. % providing a calibration check on our results. Representative spectrum of the C, O, and Si impurities are shown in Fig. 7. For both substrates, impurity doping was relatively constant although generally higher on the sapphire substrate. The interface also contains higher amounts of the three contami-

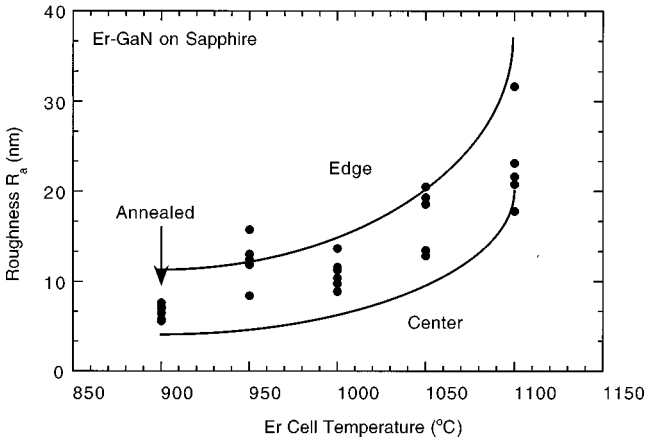

FIG. 4. Roughness measurements by AFM for GaN:Er films grown on sapphire as a function of Er cell temperature.

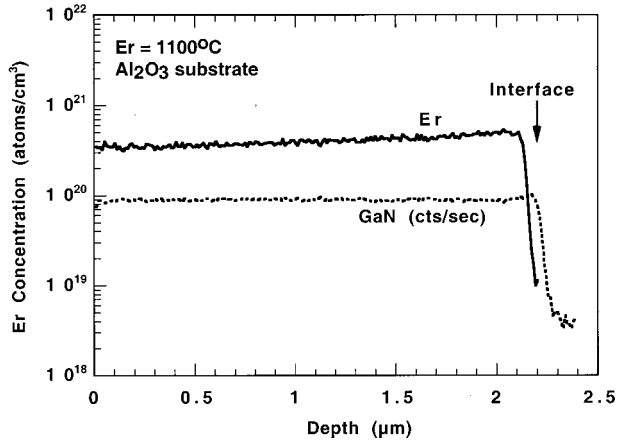

FIG. 5. Er concentration profile for a film grown on sapphire with an Er cell temperature of 1100 °C.

nants which can be remedied by a more aggressive precleaning. We believe the source of the impurities originate in the Er material. Other possible contamination avenues include the plasma source and the memory effect of the chamber. Certainly, the role of oxygen and its effect on Er PL intensity on the green and IR emission needs to be explored further. It is well known that oxygen can enhance Er emission in the IR for other semiconductors.[21–24] Typically, oxygen is doped or coimplanted with Er to achieve roughly the same or higher concentration as the rare earth. In our case, oxygen is one to two orders of magnitude lower than the Er concentration. It is also interesting to note the profile of carbon in our GaN:Er sample. Another study[25] examined the effect of carbon diffusion through an undoped layer. In that study, the authors claimed that carbon diffused throughout the undoped layer decreasing in concentration by roughly an order of magnitude. We see a similar drop in our samples (from the front surface back to the interface), yet these samples were not intentionally doped with carbon. Of course, other effects could explain the carbon profile, such as SIMS ''implantation'' of C from the contamination layer found at the top surface.

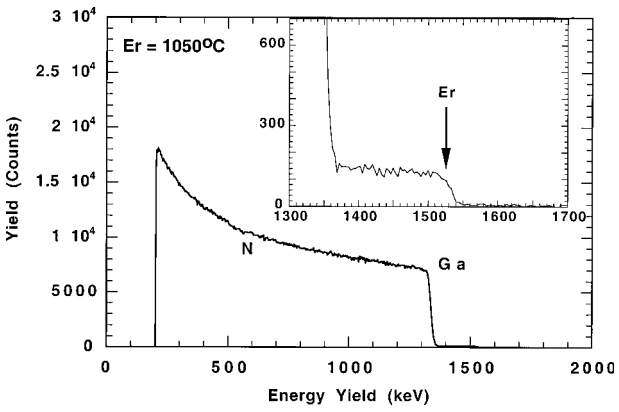

FIG. 6. RBS measurements of GaN:Er film grown on sapphire with an Er cell temperature of 1000 °C. The concentration was found to be 0.2 at. %.

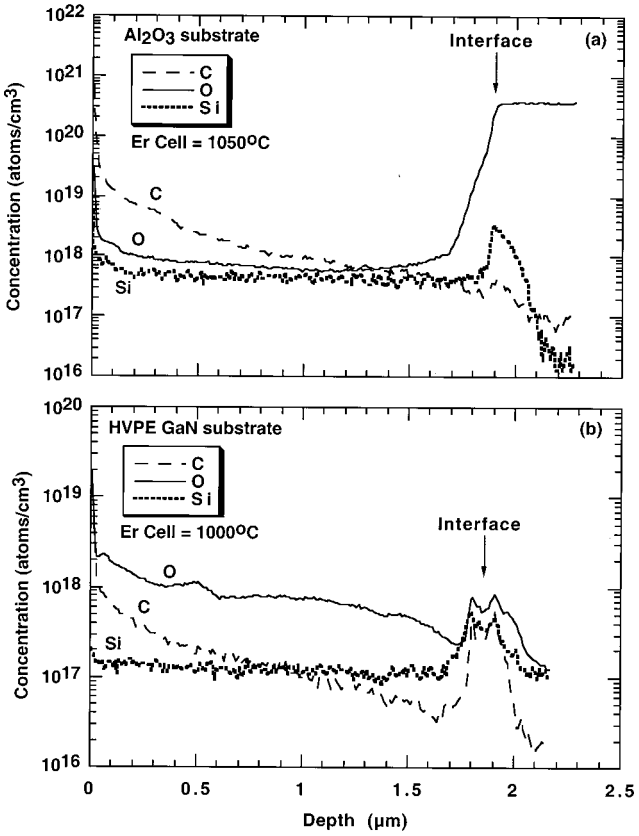

FIG. 7. SIMS measured impurity concentrations as a function of depth for films grown on sapphire (a) and HVPE GaN (b).

A plot of the Er concentration as a function of Er cell temperature for the samples grown on sapphire is shown in Fig. 8 along with the PL intensity of green (537 and 558 nm) emission lines. Generally, as the cell temperature increases, the amount of Er incorporated and thus the PL intensity increases as would be expected. From this plot we deduce that the solid solubility limit of Er incorporated in the GaN lattice has not been reached. With such a high atomic concentration of Er, we would expect some crystal defects (e.g., vacancies, dislocations, stacking faults, etc.) to be created due to the

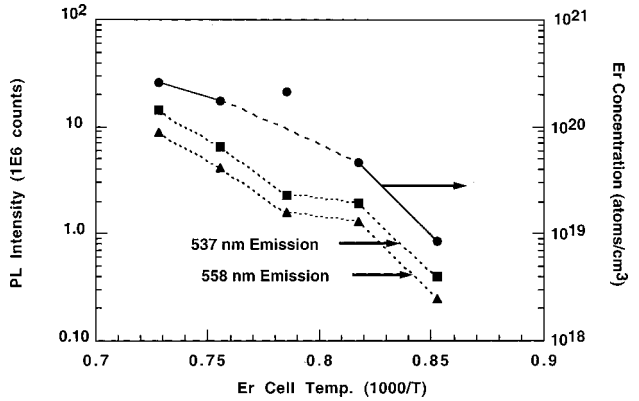

FIG. 8. Er concentration as a function of cell temperature for the samples grown on sapphire. Also shown is the PL intensity of the 537 and 558 nm Er emission lines. Lines are drawn to aid the eye.

large atomic size. Further studies need to be conducted to determine the lattice location and damage created by the heavy incorporation of such a large species.

In summary, we have reported the optical, morphological, and compositional characteristics of Er-doped GaN grown by solid source MBE on sapphire and HVPE GaN substrates. We observed novel green emission from Er in GaN and examined the corresponding structural properties of the thin films. Composition data provided by SIMS and RBS demonstrated that we have incorporated a high concentration ($\sim$1 at. %) of Er in GaN and the solubility limit had not been reached. Since emission from these films is already visible under ambient light, we expect that the intensity can be increased by higher Er incorporation. This would have significant impact for the optoelectronics industry. New and simpler devices can be manufactured that would rival existing technology.

The authors acknowledge useful discussion on SIMS analysis with A. Saleh and R. G. Wilson. This work was supported by a BMDO/ARO contract (L. Lome and J. Zavada) and a ARO AASERT grant. Equipment support was provided by an ARO URI grant and the Ohio Materials Network.

[1]A. J. Neuhalfen and B. W. Wessels, Appl. Phys. Lett. **60**, 2657 (1992).
[2]W. J. Choyke, R. P. Devaty, L. L. Clemen, M. Yoganathan, G. Pensl, and Ch. Hassler, Appl. Phys. Lett. **65**, 1668 (1994).
[3]J. M. Zavada and D. Zhang, Solid-State Electron. **38**, 1285 (1995).
[4]J. D. MacKenzie, C. R. Abernathy, S. J. Pearton, U. Hömmerich, X. Wu, R. N. Schwartz, R. G. Wilson, and J. M. Zavada, Appl. Phys. Lett. **69**, 2083 (1996).
[5]J. T. Torvik, R. J. Feuerstein, J. I. Pankove, C. H. Qiu, and F. Namavar, Appl. Phys. Lett. **69**, 2098 (1996).
[6]X. Wu, U. Hömmerich, J. D. MacKenzie, C. R. Abernathy, S. J. Pearton, R. N. Schwartz, R. G. Wilson, and J. M. Zavada, Appl. Phys. Lett. **70**, 2126 (1997).
[7]S. Kim, S. J. Rhee, D. A. Turnbull, E. E. Reuter, X. Li, J. J. Coleman, and S. G. Bishop, Appl. Phys. Lett. **71**, 231 (1997).
[8]M. Thaik, U. Hömmerich, R. N. Schwartz, R. G. Wilson, and J. M. Zavada, Appl. Phys. Lett. **71**, 2641 (1997).
[9]S. Kim, S. J. Rhee, D. A. Turnbull, X. Li, J. J. Coleman, S. G. Bishop, and P. B. Klein, Appl. Phys. Lett. **71**, 2662 (1997).
[10]S. Kim, S. J. Rhee, D. A. Turnbull, X. Li, J. J. Coleman, and S. G. Bishop, Mater. Res. Soc. Symp. Proc. **468**, 131 (1997).
[11]J. T. Torvik, C.H. Qiu, R. J. Feuerstein, J. I. Pankove, and F. Namavar, J. Appl. Phys. **81**, 6343 (1997).
[12]J. D. MacKenzie, C. R. Abernathy, S. J. Pearton, S. M. Donovan, U. Hömmerich, M. Thaik, X. Wu, F. Ren, R. G. Wilson, and J. M. Zavada, Mater. Res. Soc. Symp. Proc. **468**, 123 (1997).
[13]J. D. MacKenzie, C. R. Abernathy, S. J. Pearton, U. Hömmerich, X. Wu, R. N. Schwartz, R. G. Wilson, and J. M. Zavada, J. Cryst. Growth **175/176**, 84 (1997).
[14]D. M. Hansen, R. Zhang, N. R. Perkins, S. Safvi, L. Zhang, K. L. Bray, and T. F. Keuch, Appl. Phys. Lett. **72**, 1244 (1998).
[15]A. J. Steckl and R. Birkhahn, Appl. Phys. Lett. **73**, 1700 (1998).
[16]R. Birkhahn and A. J. Steckl, Appl. Phys. Lett. **73**, 2143 (1998).
[17]A. J. Steckl, M. Garter, R. Birkhahn, and J. Scofield, Appl. Phys. Lett. **73**, 2450 (1998).
[18]M. Garter, J. Scofield, R. Birkhahn, and A. J. Steckl, Appl. Phys. Lett. **74**, 182 (1999).
[19]M. A. Sanchez-Garcia, E. Calleja, E. Monroy, F. J. Sanchez, F. Calle, E. Munoz, and R. Beresford, J. Cryst. Growth **183**, 23 (1998).
[20]F. A. Ponce, MRS Bull. **22**, 51 (1998).
[21]J. E. Colon, D. W. Elsaesser, Y. K. Yeo, R. L. Hengehold, and G. S. Pomrenke, Appl. Phys. Lett. **62**, 216 (1993).
[22]P. N. Favennec, H. L'Haridon, D. Moutonnet, M. Salvi, and M. Gauneau, Jpn. J. Appl. Phys., Part 2 **29**, 524 (1990).
[23]P. N. Favennec, H. L'Haridon, D. Moutonnet, M. Salvi, and M. Gauneau, Mater. Res. Soc. Symp. Proc. **301**, 181 (1993).
[24]J. Michel, J. L. Benton, R. F. Ferrante, D. C. Jacobson, D. J. Eaglesham, E. A. Fitzgerald, Y. H. Xie, J. M. Poate, and L. C. Kimerling, J. Appl. Phys. **70**, 2672 (1991).
[25]B. Ya. Ber, Yu. A. Kudriavtsev, A. V. Merkulov, S. V. Novikov, D. E. Lacklison, J. W. Orton, T. S. Cheng, and C. T. Foxon, Semicond. Sci. Technol. **13**, 71 (1998).